Probing polymer chain constraint and synergistic effects in nylon 6-clay nanocomposites and nylon 6-silica flake sub-micro composites with nanomechanics

Jian Chen, Ben D. Beake, Gerard A. Bell, Yalan Tait & Fengge Gao

Published online: 16 Feb 2016.

Submit your article to this journal 🗗

View related articles 🗗

Download by: [Nottingham Trent University]   **Date:** 16 February 2016, At: 09:36

Probing polymer chain constraint and synergistic effects in nylon 6-clay nanocomposites and nylon 6-silica flake sub-micro composites with nanomechanics

Jian Chen[1], Ben D. Beake*[2], Gerard A. Bell[2], Yalan Tait[3], and Fengge Gao[3]

[1]Jiangsu Key Laboratory of Advanced Metallic Materials, School of Materials Science and Engineering, Southeast University, Nanjing 211189, China
[2]Micro Materials Ltd., Willow House, Ellice Way, Yale Business Village, Wrexham, LL13 7YL, UK
[3]School of Science and Technology, Nottingham Trent University, Clifton campus, Nottingham, NG11 8NS, UK

Abstract In this study, we report that a synergistic effect exists in the surface mechanical properties of nylon 6–clay nanocomposites (NC) that can be shown by nanomechanical testing. The hardness, elastic modulus, and nanoindentation creep behavior of nylon 6 and its nanocomposites with different filler loading produced by melt compounding were contrasted to those of model nylon 6 sub-microcomposites (SMC) reinforced by sub-micro-thick silica flakes in which constraint cannot occur due to the difference in filler geometry. Polymer chain constraint was assessed by the analysis of nanoindentation creep data. Time-dependent creep decreased with increasing the filler loading in the NC consistent with the clay platelets exerting a constraint effect on the polymer chains which increases with filler loading. In contrast, there was no evidence of any reduced time-dependent creep for the SMC samples, consistent with a lack of constraint expected due to much lower aspect ratio of the silica flakes.

Introduction

After the initial reports into clay/polymer nanocomposites,[1–6] the following years of extensive research have gradually recognized the strength and weakness of these materials. In terms of the mechanical reinforcement, this technology has advantages over traditional micro-sized fiber and filler technology at low filler contents.[7] However, as the filler content exceeds 5 wt.%, the efficiency of reinforcement of the clay/polymer nanocomposite technology can rapidly decline due to the difficulties in the exfoliation of the multi-layered structure of clay and the onset of filler agglomeration to produce small stacks of clay platelets. Although attempts have been made to produce nanocomposites with a well-ordered structure of reinforcement using pre-exfoliated clay through layer-by-layer assembly techniques,[8] the brittleness of the composites produced by this method is a barrier to many potential applications.

The mechanical properties of composites depend on the interaction of many factors, such as the filler content, its spatial distribution, and the crystallinity of the matrix, resulting in complex behavior.[9,10] In clay/nylon 6 nanocomposites, the glass transition temperature is usually unchanged or very close to that of the unfilled nylon.[6,11] It is not yet clear to what

extent the improvements in stiffness in clay/polymer nanocomposites are predominantly due to the incorporation of a much stiffer clay filler or whether the filler improves the stiffness and creep resistance by interaction with the polymer matrix exerting a constraining effect on the polymer chains. To maximize their potential, ideally NC would be designed with synergistic benefits over the base polymer, but as yet, there have been no reports that have clearly shown that such an enhancement exists and contributes to the improved surface mechanical properties. Vlasveld *et al.*[12] applied the Halpin–Tsai model originally designed for semi-crystalline polymers finding that no additional stiffening from constraint factors was necessary to explain the modulus enhancements in the clay/nylon 6 nanocomposites they studied. Understanding the relative significance of these different enhancements in mechanical properties with different processing conditions is a key step in the development of improved fabrication and processing routes capable of delivering polymer nanocomposites with optimized mechanical properties.

A recent review has highlighted that the current literature provides apparently conflicting information on the synergistic effects of polymer nanocomposites on their mechanical properties.[13] It is notable that many of the more remarkable increases in modulus in nanocomposite systems occur when the elastic modulus of the bulk polymer is very low.

*Corresponding author, email: ben@micromaterials.co.uk

Nanomechanical testing provides a convenient route to testing the mechanical behavior of novel polymer nanocomposites[14–18] since only very small volumes are required. As a surface-sensitive technique, it can provide information about surface mechanical properties more relevant to applications involving surface contact loading (e.g. sliding wear) than bulk tensile testing. In addition to the determination of mechanical properties, such as hardness (*H*) and elastic modulus (*E*), it is possible to assess time-dependent behavior[14,19–21] and the response of the composites to high-strain rate impact and repetitive contact so that fatigue can be directly studied at the nanoscale.[22] In the majority of studies[13,] there has been a focus on reporting *H* and *E* with the time-dependent behavior being an unwanted complication. However, with suitable experimental design[14,19–21] the creep behavior of the polymeric materials can be investigated at the same time as the determination of hardness and elastic modulus.

An investigation of the extent of homogeneity of the load–displacement curves and analytical treatment of the time-dependent behavior has the potential to provide information on the mechanical homogeneity and the extent of filler dispersion on finer length scales than accessible by more macro-scale techniques. Nanoindentation creep in NC has been studied previously with a range of behavior being reported.[14,23,24] The creep of layered silicate/PA6 nanocomposites has been reported to show reduced creep compared to unfilled nylon.[9,25] However, for example, Shen and co-workers found that higher nanoindentation creep in nylon 66 nanocomposites than for the base polymer.[14] Using X-ray diffraction and optical microscopy, they found a reduction in the crystal size and degree of crystallinity, concluding that morphological changes were probably the main reasons for the greater creep. Seltzer and co-workers have recently investigated the nanoindentation creep behavior of skin and core regions of injection molded samples of nylon 6/organoclay nanocomposites with 1.1–4.5 vol. % of organoclay. They found that for their samples while organoclay does improve the indentation creep resistance of nylon 6, the enhancement was solely due to a decrease in the initial creep compliance at zero time as the time-dependent creep was actually increased, i.e. in the surface/near-surface region of their NC samples probed by nanoindentation, there was no evidence of the organoclay imparting a constraining effect on the polymer chains.

We have investigated whether the finding of Seltzer *et al.* is more generally applicable by studying the nanomechanical behavior and creep response of a set of NC samples with a wider range of filler loadings from 3 to 20 wt.%. As the properties of the composites strongly depend on the filler size, composites with fillers in the sub-micro range have been investigated. Bonderer *et al.*[26] demonstrated that comprehensive reinforcement of strength, stiffness, and toughness can be achieved at relative high filler loading by applying sub-micro-thick fillers. Data from the NC samples were contrasted to a control set of nylon 6–single-layered sub-micro silica flake composites produced with the same wt.% filler loadings. During the processing, these filler in the SMC exhibited a strong reduction in aspect ratio and therefore these samples were expected to behave quite differently from the NC samples, behaving as a model system where appreciable polymer chain constraint does not occur.

In addition to charactering the properties of the NC and SMC in terms of differences in their hardness, modulus, and crystallinity, in this study, we have (i) investigated the relative importance of the initial creep compliance and time-dependent creep contributions to the total time-dependent deformation, (ii) used two different analytical methods to confirm our findings, and (iii) questioned whether nanomechanical testing can reliably produce indirect but useful information about the effectiveness of the dispersion. The results provide an improved understanding on the effects of filler size, aspect ratio, crystallinity, and content of the NC and SMC on their hardness, modulus, and creep behavior and their suitability for different applications.

Experimental

Sample preparation

The nylon 6 used for the NC and SMC composites was a high molecular weight, high viscosity nylon 6 with commercial name Grilon F50. The NC were produced by compounding with 3, 5, 10, and 20 wt.% montmorillonite clay modified with quaternary ammonium cations (commercially named as 93A) and the SMC samples were produced by compounding with 3, 5, 10, and 20 wt.% sub-micron-sized silica flake. Before composite processing, fillers and the polymer were dried under vacuum at 120 °C for 4–6 h in a vacuum oven. Then, the dried fillers were pre-blended with the polymer at different filler contents (0, 3, 5, 10, and 20 wt.%). The pre-blended materials were compounded in melt extrusion using a Prism Eurolab 16-mm twin-screw with 40/1 L/D ratio. Extruded samples were cooled in a water bath and chopped into pellets using a pelletizer. The feeding rate, screw speed, and processing temperature applied were 15–20%, 400 rpm, and 235 °C, respectively. The silica flakes were initially 350 nm thick with average aspect ratio (flake equivalent diameter to thickness ratio) of 1750 although a significant reduction of flake size occurred in the composites during processing as shown by SEM analysis of the original silica flakes before composite processing and the flakes obtained from the composites with 3wt.% and 20wt.% filler loading, respectively, by burning off the polymer matrix. During processing, the average aspect ratio of the flakes decreased from the original 1750 to 28 in the 3 wt.% SMC and 17 in the 20 wt.% SMC. The size breakdown may be caused by mechanical collision either between flakes or between flakes and the extrusion equipment during the melt processing but for our purposes is convenient in providing a range of SMC samples whose properties can be contrasted to the NC.

Crystallinity measurements

The crystallinity measurements were carried out using DSC analysis. The procedure involved: (1) heating up from −20 to 270 °C at 50 °C/min, (2) holding at 270 °C for 5 min, (3) cooling from 270 to −20 °C at 10 °C/min, (4) heating up from −20 to 270 °C at 10 °C/min, and (5) cooling from 270 to −20 °C at 50 °C/min. The first cycle of heat/cooling was aimed to remove the thermal history of the materials. The curves obtained during the temperature ramp at 10 °C/min were used to calculate the crystallinity of the materials using Equation 1:

Eqn. 1

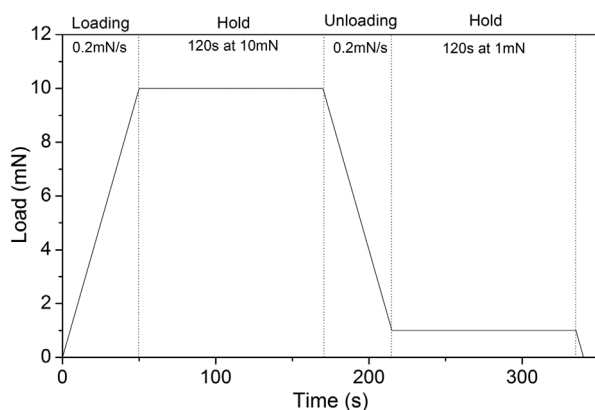$$crystallinity = {\Delta H_m}\big/{(1 - f)\Delta H_c^0}$$

Figure 1   Load vs. time protocol in the nanoindentation tests. The hold at peak load is for creep assessment and the further hold after 90% unloading is for creep recovery assessment

where ΔH_m and ΔH_c^0 represent the melt enthalpy of samples and crystallization enthalpy of 100% crystalline polymer, respectively. f is the filler mass fraction of the composite. ΔH_c^0 of 100% crystalline nylon 6 was taken as 190 J/g.

X-ray diffraction analysis of the clay and NC samples

The structure of the clay and its composites formed was characterized using X-ray diffractometry. The equipment used was an X'Pert X-ray diffractometer with Cu Kα with wavelength 1.54 nm as radiation source. Prior the experiment, the powdered clay sample was compressed into dense square-shaped tablets that could fit into the equipment sample holder. For composite samples, the materials were injection molded into square plates with dimensions 15 mm × 15 mm × 1 mm. The molded plate sample was inserted into the sample holding position directly without using a sample holder. During the experiment, the generator voltage and X-ray tube current applied were 45 kV and 40 mA, respectively. The scanning range was from 0.991º to 120º with step size 0.00835.

Nanoindentation testing

A NanoTest system produced by Micro Materials Ltd., Wrexham, UK was used for the nanoindentation testing. The system has a very high thermal stability enabling nanoindentation creep measurements to be performed without thermal drift. The experiments were conducted in an environmental enclosure controlled at 27.0 ± 0.2 °C. The humidity was ~65% RH. All samples were molded flat surfaces without polishing. The nanoindentation tests were load controlled with a Berkovich diamond indenter with the loading protocol shown in Fig. 1. The initial (contact) load was 10 μN. All the samples were loaded from this initial load to a peak load of 10 mN at a fixed loading rate of 0.2 mN s^{-1}. The load was held constant at the peak load for 120 s to record the creep response before unloading at the same rate. There was an additional 120 s hold after 90% unloading which can be used to assess the instrument drift and the sample creep recovery. For all the experiments, the rate of creep recovery was found to be almost two orders of magnitude greater than the underlying

instrumental signal drift so that the second hold period was not used for thermal drift correction. A matrix of 20 indentations spaced 100 μm apart was performed on each of the samples. The area function for the diamond indenter was determined from indentations into fused silica, although it was found that the indenter essentially indistinguishable from an ideal Berkovich geometry at the penetration depths (maximum depth ~2–3 μm) reached at 10 mN on all the samples.

The elastic modulus was determined by power law fitting to the unloading slope of the indentation curve.[27] The reduced elastic modulus, E_r, was converted to the elastic modulus, E, using the Poisson ratio for nylon 6, $\nu = 0.39$. The indentation creep behavior was analyzed in the instrument software using Equation 2.

Eqn. 2

$$\Delta d / d(0) = \left[A / d(0) \right] \cdot \ln (Bt + 1)$$

where A and B are the constants, $d(0)$ is the initial depth in the hold period, and Δd is the increase in depth during the hold period. $\Delta d/d(0)$ is the dimensionless indentation creep strain. Fitting the experimental data with Equation 2 has the benefit of (i) not requiring a particular constitutive model such as linear viscoelasticity to be assumed, therefore, allowing indentation with sharp indenters in the viscoelastic–viscoplastic regime[19,20,] (ii) being an excellent quantitative fit to the experimental creep curves enabling subtle differences in behavior to be uncovered. Equation 2 has proved successful in interpreting loading rate effects and in determination of the strain rate sensitivity, a dimensionless creep parameter that exhibits some correlation with tan delta,[20,28,29] and in determination of glass transition temperatures occurring below 0 °C.[19]

Results

Crystallinity and XRD

The crystallinity varied with filler loading in the NC and SMC samples as shown in Fig. 2a. The crystallinity of the SMC decreased significantly with only 3 wt.% loading of silica flakes and the further increase in the filler content had little effect. The crystallinity of the NC, however, increased slightly when the filler content reaching 3wt.% and then reduced significantly at higher loading. At 10 wt.%, the crystallinity of the NC was ~16%, lower than that of the SMC with the same loading.

Fig. 2b shows the XRD patterns of the organoclay 93A, nylon GF50, and its composites with 3, 5, 10, and 20 wt % organoclay 93A produced by melt processing. The organoclay clay 93A before added into the polymer has clear distinctive (001) peak at 2θ 3.81º which is equivalent to 2.316 nm interlayer spacing of silicate layers in the clay structure. However, the peak is not visible in all composite samples even in the enlarged chart in Fig. 2c.

Nanoindentation

Hardness and elastic modulus

Typical nanoindentation curves for the composites are shown in Fig. 3. The variation in elastic modulus with filler loading from analysis of such curves is shown in Fig. 4. It can clear be seen that while the NC and SMC samples were stiffer than the base polymer the enhancement in stiffness was greater for the NC samples.

The hardness and elastic modulus data are summarized in Table 1. The hardness of the nylon 6 is also increased by the incorporation of both fillers. The relative increase in hardness for the NC over the base polymer is less than the corresponding relative increase in elastic modulus. For example, incorporation of 20 wt.% clay increases the elastic modulus of nylon 6 by 150%, while the corresponding increase in hardness is only around 50%. There is greater variation in the *H* and *E* data for the composites with the sub-micron filler, especially at the higher loading. The highest average hardness was for the SMC with 20 wt.% clay.

Nanoindentation creep

The strain rate sensitivity are summarized in Table 2. Illustrative examples of the creep strain during the hold at peak load are shown in Fig. 5. While the NC show reduced creep strain compared to the matrix polymer, the SMC samples showed increased values which did not vary with filler loading.

Equation 2 was found to be an excellent fit to the creep data of NC, SMC, and the base nylon 6. The creep parameters, creep strain rate sensitivity *A/d(0)*, creep extent *A*, and time constant *1/B*, were calculated as shown in Table 2 and Fig. 6*a–c*. The *A/d(0)*, *A* and *1/B* parameters were not significantly different from those of the base polymer for the SMC, but in contrast, there was a clear decrease in all these parameters for the NC.

Discussion

As shown in Table 2, all the NC and SMC showed higher hardness and elastic modulus than the base polymer. However, the extent of this improvement was different for the NC and SMC samples. In this discussion, we aim to deconvolute the separate influences of accompanying changes in the crystallinity of the composites and the type and dispersion of the fillers on the homogeneity and enhancements in mechanical properties of the composites. A key question is whether the enhancements in stiffness are explainable without constraint. Previously at the bulk scale Vlasveld *et al*. reported that when a Halpin–Tsai model originally designed for semi-crystalline polymers is used that no additional stiffening from constraint factors was necessary to explain the modulus enhancements in the clay/nylon 6 nanocomposites, and similarly at the nanoscale, Seltzer and co-workers reported there was no evidence for constraint in the surface mechanical behavior.

Decreasing crystallinity has an adverse effect on hardness and elastic modulus.[30] Consistent with this, the mechanical properties of the lower crystallinity nylon 6 studied here are lower than those previously reported for nylon 6 with higher crystallinity.[31] For the NC, it has been reported that low loading levels (1–3 wt.%) of nanofillers can act as nucleation sites for spherulitic crystallization so that the activation energy of crystallization is lower than the matrix polymer [14]. The small increase in crystallinity observed for the 3 wt.% NC in Fig. 2 is consistent with this explanation. At higher loading levels (10–20 wt.%), the activation energy of crystallization of the nanocomposites is higher than the neat polymer as more clay particles tend to obstruct the mobilization of the polymer molecular chains, retarding crystallization and crystal growth.[32] The observed decrease in crystallinity (~30% at 10 wt.%) is that determined by Shen and co-workers by DSC.[23]

For the SMC, the crystallinity decreased to ~18 % at 3 wt.% filler and then increased slightly at 5 wt.%. Further increase in filler content has a little effect on the crystallinity as shown in Fig. 2. The sharp reduction in crystallinity in the 3 wt.% SMC appears to be due to similar reasons as NC with higher filler loading because of reduced mobility of the polymer molecules to crystallize. From this point of view, a further increase in filler content should further decrease the crystallinity due to the increased barriers to prevent crystallization. However, the progressive decrease in the aspect ratio with the increase in filler content of the SMC makes the shape of the filler more and more "roundish" as evidenced in SEM and optical microscopic studies[33] and progressively less able to influence the chain mobility of polymer molecules. As a result from these two opposing effects, further increasing filler loading did not result in a significant change in the crystallinity of the composites.

Displaying the data as relative modulus enhancement (modulus of the composites/modulus of the matrix) enables comparison between studies with different MW (and hence different stiffness) nylon 6 base materials.[6] The enhancement in stiffness, approximately doubling at 10 wt. %, is consistent with the results reviewed by Cho *et al*.,[6] and later by Vlasveld and co-workers,[12,25] Liu *et al*.,[10] Shen *et al*.[23,] and Diez-Pascual *et al*.[13] The efficiency of hardness and modulus enhancement begins to saturate at high loading levels as has been reported in previous work due to the decrease in crystallinity and a reduction in the efficiency of the exfoliation. Application of the Halpin–Tsai model can provide evidence of the effectiveness of the reinforcement with different filler loading. Following the approach taken in reference 12, the relative moduli of the fully amorphous and crystalline phases were used to estimate the elastic modulus contribution of the matrix in the nanocomposites. The Halpin–Tsai model was then used with the amorphous matrix component adjusted for the presence of surfactant to determine the effective aspect ratios of the fillers taking the density of clay = 2.8 g cm^{-3} and for silica flakes ρ = 2.2 g cm^{-3}, surfactant density = 0.93 g cm^{-3}, *E* (clay) = 172 GPa, and *E* (silica flakes) = 70 GPa. The effective aspect ratios ranged from ~210 at 3 wt.% to ~110 at 20 wt. %, consistent with the typical values of ~100–300 for layered silicate nanocomposites. The decrease in reinforcement effectiveness at higher clay, due to reduced exfoliation, is in good agreement with the literature.[12] In contrast, the values for the SMC are much lower (aspect ratios 10–60) and show little clear trend with wt.% silica flake, providing clear evidence for a marked difference in reinforcement efficiency between them and the NC.

The *H* and *E* of the composite with 5 wt.% clay were found to be lower than those of the composites with 3 wt.% clay. In a previous study involving nylon 6/organoclay NC[22,] it was found that the hardness and modulus of NC with 3 and 5% organoclay were almost identical. Shen and co-workers observed anomalous creep effects at similar loading levels on nylon 6,6 NC[14] and PEO NC samples have also shown similar behavior at 5 wt.%.[16] In all these cases, the reasons are not completely clear but it is conceivable that the structural change from the high extent of clay exfoliation state at a low content of 3 wt.% to an intercalated structure dominated state at 5 wt.% could
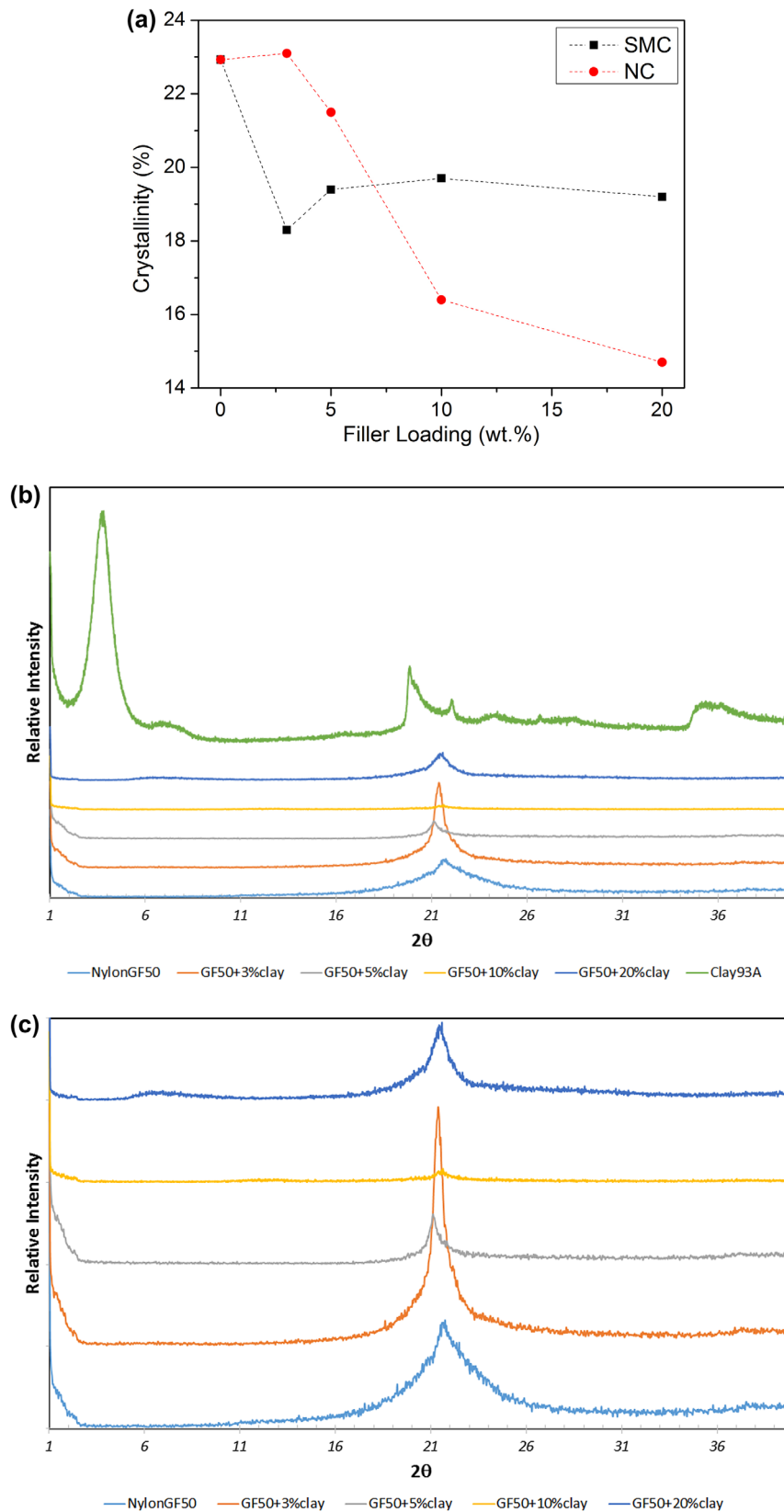
Figure 2 *a* **Variation in crystallinity with wt.% filler loading for NC and SMC** *b* **XRD patterns of the original nylon GF50, and its composites with 3, 5, 10, and 20wt% organoclay 93A, and clay 93A** *c* **enlarged view of** *b*

be associated with this phenomenon since it is well known that highly exfoliated structure with less extent of aggregation of clay in the composites is more effective in enhancing mechanical properties due to the increase in the number of effective reinforcing particles and the elimination of the weak van der Waals force between the silicate layers within a clay filler. The lower crystallinity in the 5 wt. % NC sample may also be a factor. The XRD data in Fig. 2b,c show that the clay (001)
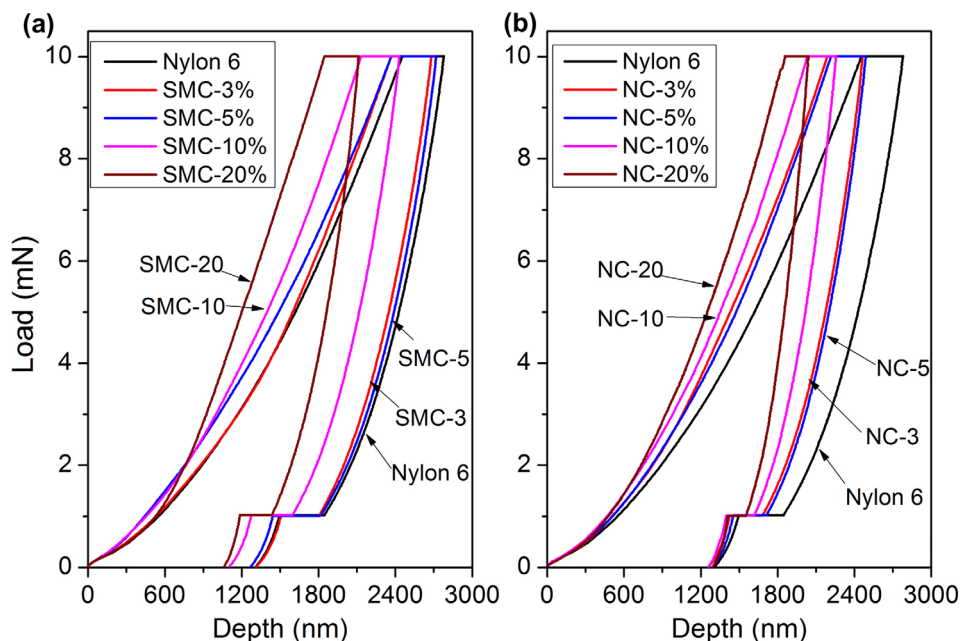
Figure 3 Typical nanoindentation curves for nylon 6 and *a* SMC and *b* NC
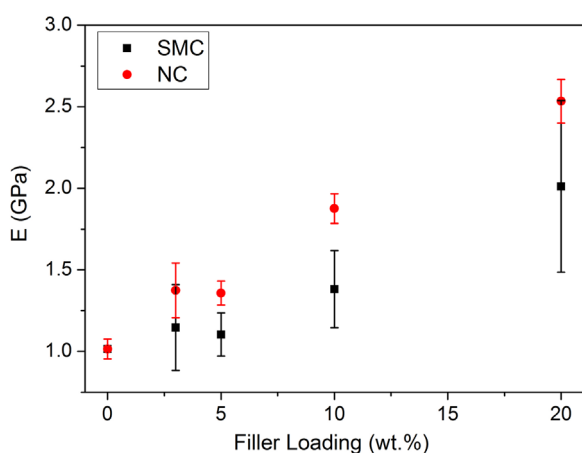

Figure 4 Variation in elastic modulus with filler loading for *a* SMC and *b* NC

peak is not clearly present in all the NC samples. This may be a limitation of the XRD technique in the effective characterization of layered structured materials when number of layers in the structure is reduced. It is reasonable to believe that a high extent of exfoliation and significant chopping down of the layered structure has occurred in all the composite materials.

Of course, this is not to say perfectly exfoliated nanocomposites have been achieved and it is likely that some intercalated structures and stacked layers with lower number of silicate layers are present that could not be detected by the XRD technique. This result is quite different from those obtained from nylon materials with medium and low molecular weight. A significant (001) peak is observed in for composites when clay loading level exceeds 5 wt % when using the same clay with medium and low molecular weight nylon 6 in the melt processing under the same experimental conditions in our laboratory. However, the nylon 6 used in the current study, Grilon F50, is a high molecular weight polymer. It is well known that the efficiency of clay exfoliation and interaction is higher when increasing molecular weight of nylon.[34]

The elastic modulus of polymeric materials can be overestimated by nanoindentation due to the continuing pronounced time-dependent deformation during unloading. This more commonly occurs when (i) the holding period is too short, (ii) and/or the loading rate is too high, (iii) and/or the indentation depth is lower than ~ 200 nm.[17,35,36] To avoid any of these artifacts influencing the measurements in this study the load vs. time protocol has been designed to (i) load sufficiently slowly (50 s), (ii) hold for a long time at peak load (120 s), and (iii) indent sufficiently deep (2–3 μm).
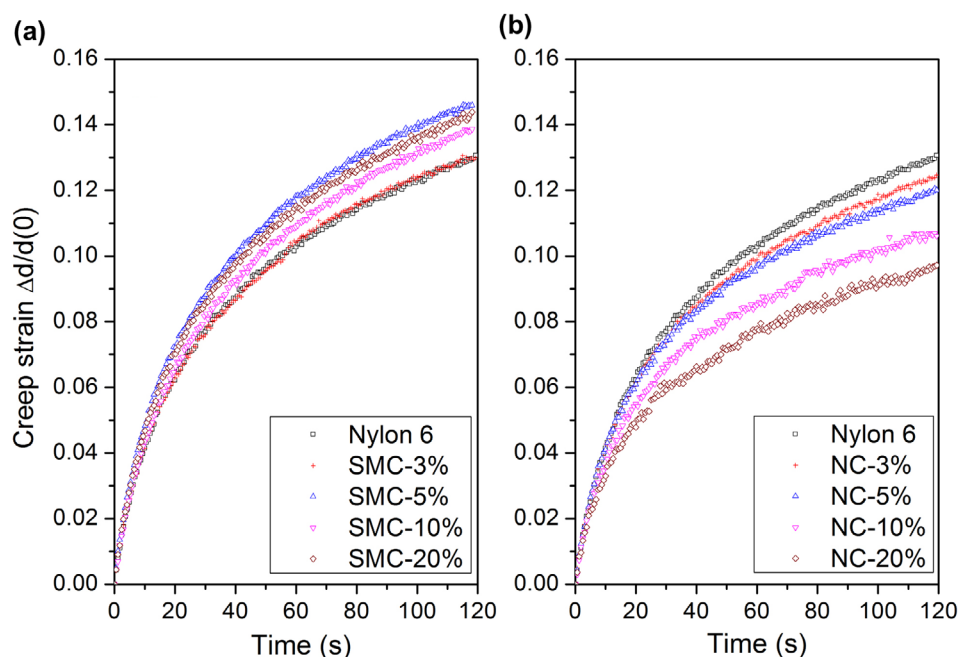
Table 1 Hardness and elastic modulus

Sample	d_{max} /nm	H/MPa	E/GPa
Nylon 6	2779 ± 106	83 ± 7	1.01 ± 0.06
SMC-3%	2688 ± 401	94 ± 27	1.15 ± 0.26
SMC-5%	2723 ± 197	86 ± 12	1.10 ± 0.13
SMC-10%	2419 ± 233	124 ± 23	1.38 ± 0.24
SMC-20%	2071 ± 333	157 ± 52	2.01 ± 0.54
NC-3%	2460 ± 189	105 ± 19	1.37 ± 0.17
NC-5%	2505 ± 74	98 ± 6	1.36 ± 0.07
NC-10%	2195 ± 76	124 ± 10	1.88 ± 0.09
NC-20%	2052 ± 101	133 ± 13	2.53 ± 0.13

Table 2 Creep and strain rate sensitivity

Sample	Strain rate Sensitivity $A/d(0)$ [*]	Creep/nm	$(1/B)$/s [*]	A/nm [*]
Nylon 6	0.043 + 0.001	319 ± 17	6.0 + 0.3	105 ± 5
SMC-3%	0.042 + 0.005	308 + 54	5.8 + 1.1	100 + 19
SMC-5%	0.046 + 0.004	330 + 34	6.2 + 0 .5	110 + 10
SMC-10%	0.045 + 0.005	287 + 51	6.2 + 0.7	95 + 14
SMC-20%	0.050 + 0.009	268 + 54	6.2 + 1.0	89 + 17
NC-3%	0.039 + 0.003	272 + 28	5.0 + 0.5	85 + 7
NC-5%	0.037 + 0.001	269 + 15	4.7 + 0.3	82 + 5
NC-10%	0.033 + 0.001	219 + 8	4.2 + 0.3	65 + 2
NC-20%	0.030 + 0.002	187 + 7	4.5 + 0.5	56 + 3

[*]Obtained by fitting the experimental creep data to Equation 2.

Figure 5 Typical creep strain curves for nylon 6 and *a* SMC and *b* NC

The significant increases in E in the composites over the nylon 6 were accompanied by a smaller rise in H. In a previous study involving nylon 6/organoclay NC[22,] it was found that although the stiffness of 3 and 5 wt. % organoclay was over 20% greater than nylon 6 the hardness of the NC did not change. Consequently, the H/E in the composites is lower than in the matrix polymer. The change in H/E may have important implications for tribological applications where performance often is correlated with parameters such as H/E and H^3/E^2, with higher H^3/E^2 commonly resulting in a higher load for non-elastic deformation, and higher wear resistance to wear as has been achieved by cross-linking ultra-high molecular weight polyethylene (UHMWPE) for replacement of hip prostheses.[37] The tribology and wear of polymers and polymer-based composites is complicated by viscoelastic recovery and brittleness,[38–40] with Brostow and co-workers reporting a direct correlation between a brittleness index and scratch recovery.[40] Although wear resistance may improve by adding silicate layers to nylon 6, this has been associated with an increase in brittle modes of deformation such as the formation of brittle cracks during scratching.[41] A reduction in H/E when compared to matrix polymers has been reported previously for nylon 6 with 3–5% organoclay and for PEO with 7–15%

organoclay.[22] In the current study, the decrease in H/E is more marked for the NC than the SMC as shown in Fig. 7. As the hardness is determined from the unloading curve after creep it is important to consider the influence of the reduced creep on its determination. Increased hardness in NC in comparison to nylon 6 is partially due to the reduction in creep. At 3 and 5% filler, the increased hardness of the NC is consistent with their greater creep resistance. For the higher loadings, the more rapid increase in hardness on the SMC samples is more likely to be connected to the increase in crystallinity with creep acting to minimize the difference.

Indentation creep analysis

With high-thermal stability instrumentation and suitable experimental design, the analysis of nanoindentation creep data can provide detailed information on the ability of the fillers to constrain the polymer chains in the composites. Nanoindentation of NC is commonly either load or strain rate-controlled, with a load ramp terminated at a set indenter penetration depth. However, it has been shown[20] that the analysis of indentation creep is aided by the choice of a *constant loading time* rather than the use of (i) a depth-terminated load
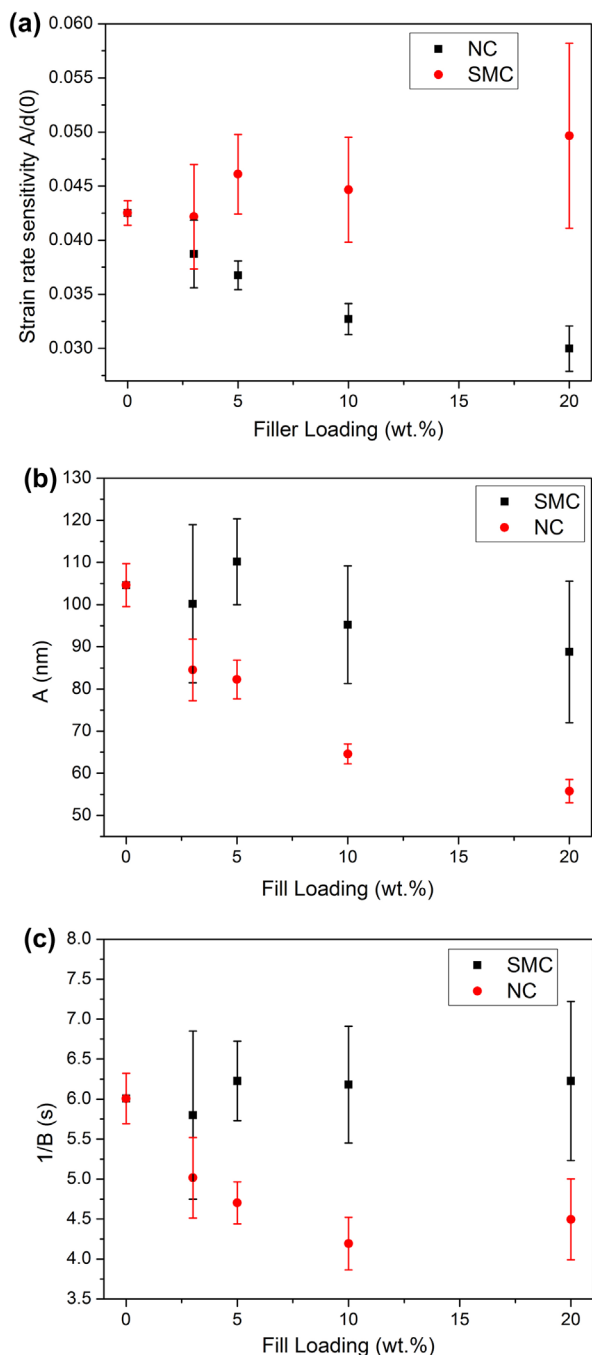
(a)

(b)

(c)

Figure 6 Variation in the *a* **strain rate sensitivity** *A/d(0)*, *b* **creep extent parameter** *A*, **and** *c* **time constant** *1/B*

Figure 7 Variation in *H/E* with filler loading for *a* **SMC and** *b* **NC**

and semi-crystalline polymers have shown that minimum values of the time constant 1/*B* are observed close to the glass transition region.[29] More recently[19,] the treatment has been applied to analyze sub-ambient temperature nanoindentation creep data of atactic polypropylene and observe a minimum in time constant 1/*B* in the vicinity of the glass transition region more clearly than the maximum in *A/d(0)* at the same temperature. The SMC showed much improved *H* and *E* than the matrix but without any clear variation in creep parameters in the composite as compared with the nylon 6 as shown in Table 2 and Fig. 6, consistent with no synergistic constraint in the SMCs.

In contrast, the creep parameters for the clay nanocomposites decrease compared nylon 6 and continue to fall as filler loading increases. Previous studies on the creep of layered silicate/PA6 nanocomposites have shown reduced creep compared to unfilled nylon.[9,25] Interestingly, Seltzer and co-workers[9] investigated the creep properties of their organoclay-enhanced PA6 nanocomposites using both nanoindentation and cantilever bending. In nanoindentation, the nanocomposites showed increased creep resistance which is in agreement with our findings on NC and SMC. To separate out the relative effects of initial creep compliance and time-dependent creep, the data were normalized by the initial creep compliance. To enable comparison with their work, the time-dependent creep compliance, $(J_{app}-J_0)/J_0$, was also determined using their proposed method according to Equation 3.[21]Eqn. 3

$$(J_{app} - J_0)/J_0 = \left(d/d(0)\right)^2 - 1$$

where *d* is the penetration depth. The time-dependent creep is shown in Fig. 8 which shows the same trends as the creep strain curves as shown in Fig. 5. This finding contrasts with the same analysis of the time-dependent creep during nanoindentation by Seltzer *et al*.[9] who found that it was larger for all their NC sample than for the matrix. This result is similar to that reported herein for the SMC composites (where no constraint was expected or found) and implies differences in the surface structure of the NC produced by Seltzer *et al*. In contrast to their behavior in nanoindentation, in bulk measurements by cantilever bending[9,] they observed reduced time-dependent

history, (ii) constant loading rate experiments to different peak loads, or (iii) constant strain (proportional loading), as in all of these cases the changing time taken to reach the peak load influences the creep behavior, making a robust analytical comparison between samples more problematic. By employing the same 50 s loading ramp for all the samples, the current study has made it possible to observe small but clear changes in strain rate sensitivity and time constant.

The creep strain rate sensitivity, *A/d(0)*, and time constant 1/*B*, are sensitive to viscoelastic behavior.[19,29] The experimental creep depth data are closely fitted by the logarithmic Equation 2 enabling subtle changes in behavior to be determined. Tests at room and elevated temperatures on a range of amorphous
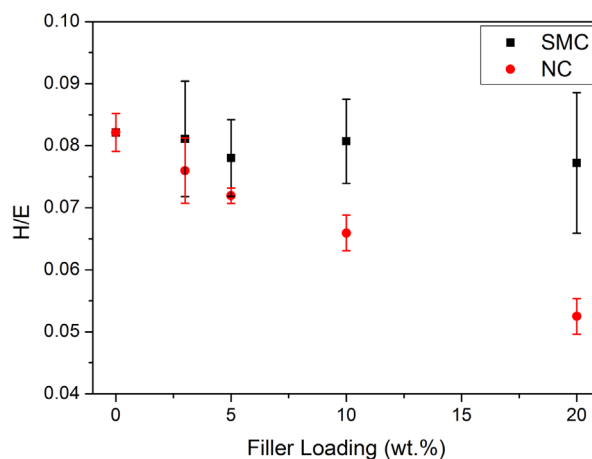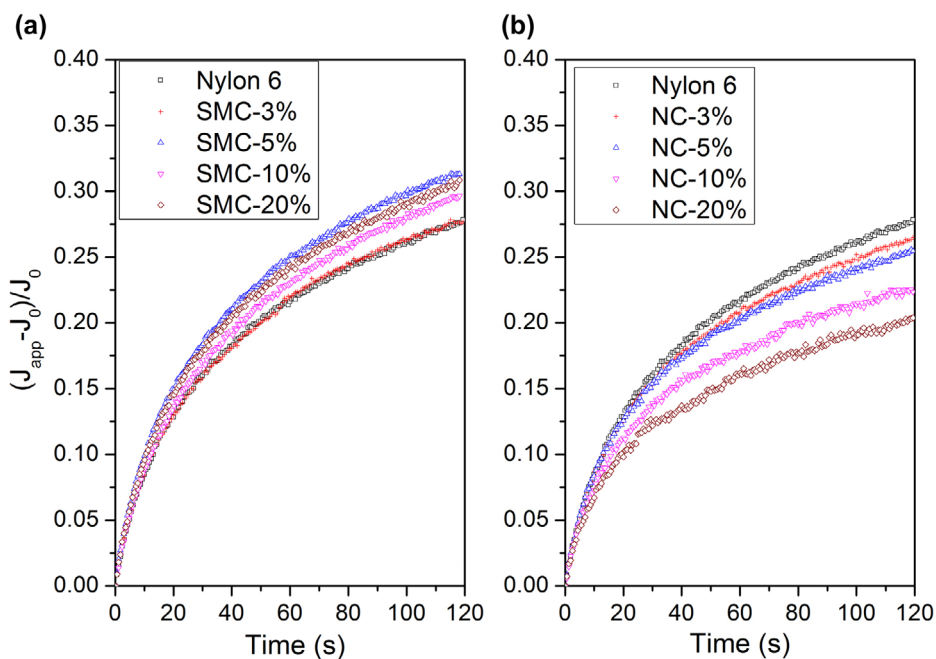
(a)

(b)

Figure 8   Variation in time-dependent creep with filler loading for *a* SMC and *b* NC

behavior in the composites and therefore suggested that the organoclay imparts a constraint effect on the PA 6 molecular chains, restricting their mobility in the bulk compared to the surface.

In our analysis of the nanoindentation creep on NC, reduced initial creep compliance *and* time-dependent creep were found to contribute to the improvement in creep resistance. The strain rate sensitivity approach (Equation 2) also clearly shows this difference in the time-dependent component. As a further confirmation, we reanalyzed indentation creep data in our laboratory on stiffer nylon 6 NC samples with 3–5% organoclay (hardness and modulus data previously reported in ref[22]). The analysis also revealed reduced strain rate sensitivity (Equation 2) and time-dependent creep (Equation 3) in the nanocomposites in comparison to nylon 6. The analysis of the data shows that some constraint does indeed occur. Smaller but still significant rises in stiffness can be observed (e.g. ~40% increase for 10 wt. % SMC and ~100% increase at 20 wt. % SMC) for systems without constraint.

Conclusions

The results show that NC are more effective in enhancing stiffness and creep behavior in nylon 6 than in the SMC composites despite the larger decrease in crystallinity that occurs for the former. The analysis of nanoindentation creep data appears to be a very effective approach for assessing the presence of surface/near-surface constraint of the polymer by clay platelets or silica flakes. The creep analysis showed that both reduced initial creep compliance and time-dependent creep contribute to the improved creep resistance of NC implying that the clay has a beneficial constraining effect on the polymer chains in the nanocomposites. This new finding is in contrast to the creep behavior of nylon 6–silica flake SMC studied here and to that of nylon 6/organoclay nanocomposites reported in[9] where improved indentation creep was found to only be due

to the improved initial creep compliance, and constraint did not occur.

The methodology applied in this study has provided strong evidence that constraint does occur in nylon 6–clay nanocomposites and could prove a valuable tool in their future optimization. It is also easily applicable to other systems such as CNT/polymer nanocomposites.

Conflicts of interest

The authors have no conflicts of interest to declare.

References

1. Y. Kojima, A. Usuki, M. Kawasumi, A. Okada, Y. Fukushima, T. Kurauchi and O. Kamigaito: *J. Mater. Res.*, 1993, **8**, 1185–1189.
2. A. Usuki, Y. Kojima, M. Kawasumi, A. Okada, Y. Fukushima, T. Kurauchi and O. Kamigaito: *J. Mater. Res.*, 1993, **8**, 1179–1184.
3. A. Usuki, M. Kawasumi, Y. Kojima, A. Okada, T. Kurauchi and O. Kamigaito: *J. Mater. Res.*, 1993, **8**, 1174–1178.
4. R. A. Vaia and E. P. Giannelis: *Macromolecules*, 1997, **30**, 7990–7999.
5. M. Kawasumi, N. Hasegawa, M. Kato, A. Usuki and A. Okada: *Macromolecules*, 1997, **30**, 6333–6338.
6. J. W. Cho and D. R. Paul: *Polymer*, 2001, **42**, 1083–1094.
7. F. Gao: *Mater. Today*, 2004, **7**, 50–55.
8. P. Podsiadlo, A. K. Kaushik, E. M. Arruda, A. M. Waas, B. S. Shim, J. Xu, H. Nandivada, B. G. Pumplin, J. Lahann, A. Ramamoorthy and N. A. Kotov: *Science*, 2007, **318**, 80–83.
9. R. Seltzer, Y. Mai and P. M. Frontini: *Composites Part B: Engineering Nanomechanics and Nanocomposites: Mechanical Behavior*, 2012, **43**, 83–89.
10. T. X. Liu, Z. H. Liu, K. X. Ma, L. Shen, K. Y. Zeng and C. B. He: *Compos. Sci. Technol.*, 2003, **63**, 331–337.

11. D. Vlasveld, J. Groenewold, H. Bersee and S. J. Picken: *Polymer*, 2005, **46**, 12567–12576.
12. D. Vlasveld, J. Groenewold, H. Bersee, E. Mendes and S. J. Picken: *Polymer*, 2005, **46**, 6102–6113.
13. A. M. Díez-Pascual, M. A. Gómez-Fatou, F. Ania and A. Flores: *Prog. Mater. Sci.*, 2015, **67**, 1–94.
14. L. Shen, I. Y. Phang, L. Chen, T. X. Liu and K. Y. Zeng: *Polymer*, 2004, **45**, 3341–3349.
15. J. Chen, X. L. Guo, Q. Tang, C. Y. Zhuang, J. S. Liu, S. Q. Wu and B. D. Beake: *Carbon*, 2013, **55**, 144–150.
16. B. D. Beake, S. Chen, J. B. Hull and F. Gao: *J. Nanosci. Nanotech.*, 2002' **2**, 73–79.
17. D. Tranchida, S. Piccarolo, J. Loos and A. Alexeev: *Macromol.*, 2007, **40**, 1259–1267.
18. A. Dasari, Z. Z. Yu and Y. W Mai: *Mater. Sci. Eng. R.*, 2009, **63**, 31–80.
19. J. Chen, G. A. Bell, H. S. Dong, J. F. Smith and B. D. Beake: *J. Phys. D: Appl. Phys.*, 2010, **43**, 425404.
20. B. Beake: *J. Phys. D: Appl. Phys.*, 2006, **39**, 4478–4485.
21. R. Seltzer and Y. Mai, *Eng. Fract. Mech.*, 2008, **75**, 4852–4862.
22. B. D. Beake, S. R. Goodes, J. F. Smith and F. Gao: *J. Mater. Res.*, 2004, **19**, 237–247.
23. L. Shen, I. Y. Phang, T. X. Liu and K. Y. Zeng: *Polymer*, 2004, **45**, 8221–8229.
24. L. Shen, W. C. Tjiu and T. Liu: *Polymer*, 2005, **46**, 11969–11977.
25. D. P. N. Vlasveld, H. E. N. Bersee and S. J. Picken: *Polymer*, 2005, **46**, 12539–12545.
26. L. J. Bonderer, A. R. Studart and L. J. Gauckler: *Science*, 2008, **319**, 1069–1073.
27. W. C. Oliver and G. M. Pharr: *J. Mater. Res.*, 1992, **7**, 1564–1583.
28. A. Gray and B. D. Beake: *J. Nanosci. Nanotech.*, 2007, **7**, 2530–2533.
29. A. Gray, D. Orecchia and B. D. Beake: *J Nanosci. Nanotech.*, 2009, **9**, 4514–4519.
30. B. D. Beake and G. J. Leggett: *Polymer*, 2002, **43**, 319–327.
31. G. A. Bell, D. M. Bieliński and B. D. Beake: *J Appl. Poly. Sci.*, 2008, **107**, 577–582.
32. W. R. Broughton: 'Characterization of nanosized filler particles in polymeric systems: a review', NPL Report MAT12; 2008, Teddington, UK, NPL.
33. Y Li, PhD thesis: 'The development of sub-micro filler enhanced composites', Nottingham Trent University, UK, Nov 2007.
34. T. D. Fornes, P. J. Yoon, H. Keskkula and D. R. Paul: *Polymer*, 2001, **42**, 9929–9940.
35. C. A. Tweedie, G. Constantinides, K. E. Lehman, D. J. Brill, G. S. Blackman and k. J. Van Vliet, Adv. Mater., 2007, **19**, 2540.
36. D. Tranchida, S. Piccarolo, J. Loos and A. Alexeev: Appl. Phys. Lett., 2006, **89**, 171905.
37. P. A. Williams, K. Yamamoto, T. Masaoka, H. Oonishi and I. C. Clarke: Tribol. Trans., 2007, **50**, 277–290.
38. W. Brostow, J. –L. Deborde, M. Jaklewicz and P. Olszynski: J. Mater. Ed., 2003, **25**, 119–132.
39. N. K. Myshkin, M. I. Petrokovets and A. V. Kovalev: Tribol. Int., 2005, **38**, 910–921.
40. W. Brostow, V. Kovacevic, D. Vrsaljko and J Whitworth: J. Mater. Ed., 2010, **32**, 273–290.
41. D. Aravind and Z. Yu: *Nanotechnol.*, 2008, **19**, 55708.